Citation: Abin-Fuentes, A., M. E.-S. Mohamed, D. I. C. Wang, and K. L. J. Prather. "Exploring the Mechanism of Biocatalyst Inhibition in Microbial Desulfurization." Applied and Environmental Microbiology 79, no. 24 (October 4, 2013): 7807–7817.

As Published: http://dx.doi.org/10.1128/aem.02696-13

Publisher: American Society for Microbiology

Persistent URL: http://hdl.handle.net/1721.1/92419

Version: Author's final manuscript: final author's manuscript post peer review, without publisher's formatting or copy editing

Massachusetts Institute of Technology

Exploring the mechanism of biocatalyst inhibition in microbial desulfurization

Andres Abin-Fuentes[1], Magdy El-Said Mohamed[2], Daniel IC Wang[1] and Kristala LJ Prather[1*]

[1]Department of Chemical Engineering, Massachusetts Institute of Technology, Cambridge, MA, 02139, USA

[2]R&DC, Saudi Aramco, Dhahran 31311, Saudi Arabia

*author to whom correspondence should be directed

T: 617-253-1950, e-mail: kljp@mit.edu

15   **Abstract**

16   Microbial desulfurization or biodesulfurization (BDS) of fuels is a promising technology because

17   it can desulfurize compounds that are recalcitrant to the current standard technology in the oil

18   industry. One of the obstacles to the commercialization of BDS is the reduction in biocatalyst

19   activity concomitant with the accumulation of the end product 2-hydroxybiphenyl (HBP) during

20   the process. BDS experiments were performed by incubating *Rhodococcus erythropolis* IGTS8

21   resting cell suspensions with hexadecane at 0.50 vol/vol containing 10 mM dibenzothiophene.

22   The resin Dowex® Optipore SD-2 was added to the BDS experiments at resin concentrations of

23   0, 10 or 50 g-resin/L-total. The HBP concentration within the cytoplasm was estimated to

24   decrease from 1100 to 260 μM with increasing resin concentration. Despite this finding,

25   productivity did not increase with resin concentration. This led us to focus on the susceptibility

26   of the desulfurization enzymes towards HBP. Dose-response experiments were performed to

27   identify major inhibitory interactions in the most common BDS pathway, the 4S pathway. HBP

28   was responsible for three of the four major inhibitory interactions identified. The concentrations

29   of HBP that led to 50% reduction in the enzymes' activities (IC_{50}) for DszA, DszB and DszC

30   were measured to be 60 ± 5 μM, 110 ± 10 μM and 50 ± 5 μM, respectively. The fact that the

31   IC_{50} values for HBP are all significantly smaller than the cytoplasmic HBP concentration

32   suggests that the inhibition of the desulfurization enzymes by HBP is responsible for the

33   observed reduction in biocatalyst activity concomitant with HBP generation.

34   Keywords: Enzyme inhibition, *Rhodococcus erythropolis* IGTS8, biodesulfurization,

35   dibenzothiophene, 2-hydroxybiphenyl

Introduction

Biodesulfurization (BDS) is a process in which microorganisms, typically bacteria, are used to reduce the level of sulfur in fuels derived from crude oil including diesel and gasoline. BDS has gained interest over the last 20 years as an alternative to hydrodesulfurization (HDS), which is the current desulfurization standard in the oil industry. HDS uses a metal catalyst along with hydrogen gas (H_2) at high temperature and pressure to remove sulfur from organic sulfur compounds and generate H_2S gas (1). Major drawbacks of HDS include steric hindrance of the metal catalysts by certain recalcitrant compounds and large energy consumption due to process operation at high temperature and pressure (1). Recalcitrant compounds include the parent molecule dibenzothiophene (DBT) and some of its alkylated derivatives, such as 4-methyldibenzothiophene (4-DBT) and 4,6-dimethyldibenzothiophene (4,6-DBT). BDS can potentially be used to remove the sulfur that cannot be removed by HDS, though it is likely not a replacement for the current HDS infrastructure. The use of more than one desulfurization technology may be necessary to meet the increasingly stringent sulfur regulations (1).

There is a wide range of microorganisms known to have BDS capability (2). Such microorganisms typically desulfurize DBT by one of two pathways: the Kodama pathway or the 4S pathway (1). The Kodama pathway is a destructive BDS pathway in which carbon-carbon bonds in the DBT molecule are broken and sulfur is not selectively removed from the organic molecule. Due to its destructive nature, the Kodama pathway reduces the caloric value of the fuel that is being desulfurized. As a result, the majority of the focus on the past 20 years has been on the 4S pathway, which is an oxidative desulfurization pathway that cleaves the carbon-sulfur bond in DBT and leaves the carbon structure intact. The 4S pathway is a four-step enzymatic pathway that converts DBT to 2-hydroxybiphenyl (HBP) and sulfate (Figure 1). The

59   first two steps are the conversion of DBT to DBT-sulfoxide (DBTO) and then to DBT-sulfone

60   (DBTO$_2$). These steps are catalyzed by the enzymes DszC monooxygenase and DszD

61   oxidoreductase in synchrony. The third step is the conversion of DBTO$_2$ to 2-(2′-hydroxyphenyl)

62   benzene sulfinate (HBPS), which is catalyzed by DszA monooxygenase and DszD

63   oxidoreductase in synchrony. The final step is the conversion of HBPS to HBP and sulfite by

64   DszB desulfinase (3).

65   The isolation and purification of the desulfurization enzymes from *R. erythropolis* IGTS8

66   has been reported (4, 5). Preliminary characterization of these enzymes showed that DszB

67   catalyzes the slowest reaction with a turnover number (k_{cat}) of "about 2 min^{-1}" (4). Furthermore,

68   it was reported that DszA "has a turnover number (k_{cat}) of about 1/sec" (4). Following the

69   finding that DszB catalyzes the slowest step, the kinetics of DszB was investigated in detail (6).

70   DszB kinetics was modeled appropriately by the Michaelis-Menten model with a Michaelis

71   constant (K_m) of 0.90 ± 0.15 μM and a k_{cat} of 1.3 ± 0.07 min^{-1} (6). The kinetics of DszA, DszC,

72   and DszD from *R. erythropolis* IGTS8 have yet to be investigated in detail.

73   Two major obstacles facing BDS commercialization are that: (1) biocatalyst activities are

74   significantly lower than what is needed for BDS rates to match HDS rates (2); and (2)

75   biocatalysts cannot maintain activity for a long period of time. Considerable effort has gone into

76   trying to understand and overcome the limitations to the desulfurization activity of the

77   biocatalysts. Several studies have shown that genetic engineering can lead to higher

78   desulfurization activities (2). For example, the desulfurization activity of *R. erythropolis* KA2-5-

79   1 was increased from 50 to 250 μmol DBT/g DCW/h by providing multiple copies of the

80   desulfurization genes and placing them under the control of alternative promoters (2).

81   Reduction in biocatalyst activity over time has been widely reported in BDS processes (2,

82   7, 8). The reduction in activity is typically correlated to the accumulation of HBP in the

83   medium during the BDS process. The desulfurization activity of a cell suspension of *R.*

84   *erythropolis* IGTS8 of cell density 66 g DCW/L mixed with hexadecane (at 1:1 v/v ratio)

85   containing 19000 μM DBT was found to follow first order decay with decay constant of 0.072 h^{-}

86   ^{1} (7). It was suggested that the loss of biocatalyst activity might be due to exposure to increasing

87   HBP concentrations, although no experiments were done to validate this hypothesis (7). The

88   cells were active for 24 hours and only 7000 out of 19000 μM DBT in oil was consumed. The

89   final concentration of HBP accumulated in the oil phase after 24 hours was only 3300 μM.

90   Although aqueous phase accumulation of DBT or HBP was not measured, the contribution from

91   the aqueous phase concentration to the overall concentration of either compound could not have

92   been more than 5%. This was estimated based on the partition coefficients of DBT and HBP

93   between hexadecane and water ($P_{O/W}$), which are 21000 and around 30-50, respectively (9). As a

94   result, approximately 3600-3700 μM of DBT or HBP are unaccounted for at the end of the BDS

95   process. Possible reasons for the discrepancy between DBT disappearance and HBP

96   accumulation are accumulation of pathway intermediates or retention of DBT and/or HBP within

97   the biocatalyst. *R. erythropolis,* being a gram-positive bacteria, has a cytoplasmic membrane

98   surrounded by a thick cell wall made mostly of peptidoglycan. The cell wall is composed of

99   thick peptidoglycan structure to which fatty acid molecules are attached. In the case of *R.*

100   *erythropolis* (a member of the actinomycetes family), the cell wall is composed of mycolic acids

101   that are perpendicular to the cell surface (10). These mycolic acids range from 30 to 54 carbon

102   atoms in length and they make the cell wall of *R. erythropolis* highly hydrophobic. It is possible

103   that a significant concentration of DBT initially in the oil phase would have been retained within

104   the cell wall of *R. erythropolis* IGTS8 as it entered the cell. It is also possible that a significant

105 fraction of HBP produced by the biocatalyst would have been trapped within the biocatalyst

106 cytoplasmic membrane or cell wall as it exited the cell. The amount of DBT or HBP retained by

107 the biocatalyst will depend on the partition coefficients between the biocatalyst and the oil or

108 aqueous phases, $P_{C/O}$ or $P_{C/W}$, respectively.

109   A number of studies have investigated the effect of HBP on biocatalyst activity. HBP has

110 been shown to inhibit the growth of *R. erythropolis* IGTS8 at concentrations greater than 200 μM

111 (11). Preliminary characterization of the DszB enzyme from *R.erythropolis* KA2-5-1 showed

112 that its activity is reduced by 50% at HBP concentrations around 2000 μM (12). In other studies,

113 the effect of exogenously added HBP on the BDS process has been described. *R. erythropolis*

114 IGTS8 aqueous resting cell suspensions of 2 g DCW/L were prepared and supplied with only

115 one of the 4S pathway compounds (either DBT, DBTO, DBTO$_2$ or HBPS) (13). HBP was also

116 added at concentrations of either 0 and 50 μM in each experiment. The disappearance rate of

117 each compound was monitored over a short period of 15 min. It was found that the

118 disappearance rates of DBTO and HBPS were significantly reduced by the presence of 50 μM

119 HBP. These results suggested that HBP might be inhibitory to the enzymes responsible for

120 DBTO and HBPS consumption, which are DszC and DszB, respectively (Figure 1). In a

121 different study, the DBT desulfurization rate of resting cells of *Microbacterium* sp. ZD-M2 was

122 found to decrease significantly when HBP was added exogenously at concentrations ranging

123 from 0-2000 μM (14). Results from experiments where HBP is added exogenously cannot be

124 used to quantitatively predict the effect of HBP on a typical BDS process where DBT is added

125 exogenously and HBP is generated endogenously within the cytoplasm of the cells. When HBP

126 is added exogenously, a significant fraction may be retained by the cell wall and may never reach

127 the cytoplasm, where inhibition of the desulfurization enzymes could occur. On the other hand,

128   HBP generated endogenously within the cytoplasm is immediately at the location where it can be

129   inhibitory to the desulfurization enzymes. Therefore, the specific HBP loading of the biocatalyst

130   (mg HBP/g DCW) that leads to a certain level of reduction in BDS activity may be significantly

131   larger when HBP is added exogenously.

132   In summary, there is sufficient evidence to suggest that HBP (either generated

133   endogenously or supplied exogenously) reduces the overall biocatalyst activity. In this work, a

134   series of commercially available adsorbents were screened for their affinity and selectivity to

135   adsorb HBP. The best adsorbent was used to determine whether or not HBP selective adsorbents

136   could help mitigate the loss of desulfurization activity correlated with HBP accumulation during

137   the BDS process. The kinetics and inhibition of the four enzymes in the 4S pathway by the

138   intermediate compounds were next investigated in detail, in an attempt to understand the

139   mechanism for the reduction in biocatalyst activity that is correlated with HBP accumulation.

140

141   **Materials and Methods**

142   *Bacterial strains, vectors, media and chemicals.* The DBT-desulfurizing strain used in this study

143   was *Rhodococcus erythropolis* IGTS8 ATCC® 53968[TM], purchased from the American Type

144   Culture Collection (USA). The defined minimal medium (MM) for cultivation contained (per

145   liter of deionized water): glucose 30.0 g, NH_4Cl 3.0 g, $K_2HPO_4.3H_2O$ 6.75 g, $NaH_2PO_4.H_2O$ 2.25

146   g, $MgCl_2$ 0.245 g, $FeCl_3$ 4 mg, $CaCl_2$ 4 mg, Na_2SO_4 0.14 g, $ZnCl_2$ 32 mg, $MnCl_2.4H_2O$ 1 mg,

147    $CuCl_2.2H_2O$ 5 mg, $Co(NO_3)_2.6H_2O$ 0.7 mg, $Na_2B_4O_7.10H_2O$ 0.7 mg, $(NH_4)_6Mo_7O_{24}.4H_2O$ 1 mg,

148   EDTA 12 mg. Cryogenic stocks were prepared by addition of 15% (vol./vol.) glycerol (final

149   concentration) to mid-log growth phase cultures in MM, which were then kept at -80°C for long

150   term storage. Medium components were obtained from VWR International (USA). Dr.

151   Christine Nguyen, from Professor Stephen Buchwald's research group at MIT, kindly provided

152   HBPS. All other chemicals were obtained from Sigma-Aldrich (USA). The strains used for

153   expression of the desulfurization genes were *Escherichia coli* MAX Efficiency® DH10B[TM] and

154   *E. coli* BL21 Star[TM] (DE3) One Shot® from Invitrogen[TM]. The vector used for all molecular

155   manipulations was pETDuet-1 from Novagen®. The medium used to culture these strains was

156   Luria-Bertani (LB) broth from DIFCO® supplemented with ampicillin (100 μg/ml working

157   concentration) for selection of clones containing the pETDuet-1 vector.

158

159   *Testing HBP adsorbents.* Activated charcoal, molecular sieves (of 4, 5, and 13 Å pores),

160   Diaion® HP-20, Dowex® Optipore L-493, SD-2, Biobeads, Amberlite® XAD4, IRC86, IRA958

161   were all obtained from Sigma-Aldrich (USA). Resins were tested for their ability to adsorb HBP

162   from a hexadecane-water solution. The adsorption experiments were carried out in 20 mL

163   scintillation vials by mixing 5 mL of water with 5 mL of a hexadecane solution containing 10000

164   μM DBT and 10000 μM HBP with either 0.1 or 1.0 g of resin. Mixtures were equilibrated for 24

165   h at 30°C, with agitation at 250 rpm. After measuring solute concentrations before and after

166   sample equilibration with a particular resin concentration (X_r), specific loadings (L_r) were

167   determined by the following relationships:

168   $$X_r = \frac{m_r}{V_{total}}$$ (1)

169   $$L_r = \frac{\left(C_{HBP}\big|_{t_0} - C_{HBP}\big|_{t_{eq}}\right)MW_{HBP}}{X_r},$$ (2)

170   where C_{HBP} represents the total concentration of HBP (in oil and water), V_{total} is the total volume

171   of solution (oil plus water), m_r is the mass of resin used, X_r is the concentration of resin

8

172   employed, MW_{HBP} is the molecular weight of HBP (170 g/mole), and t_0 and t_{eq} represent time at

173   initial and equilibrium conditions, respectively.

174

175   *Resting cells preparation.* *R. erythropolis* IGTS8 cultures were grown in 400 mL of MM in a 2L

176   shake flask for a period of 40-48 hours during which the cell density increased from

177   approximately 0.03 g DCW/L to 3 g DCW/L. Cultures were centrifuged at 5000 RPM and 4°C

178   for 15 min and spent media was discarded. Biocatalyst pellets were resuspended to the

179   experimental cell density in 5 g/L glucose and 20 mM phosphate buffer pH 7.0.

180

181   *Four-component biodesulfurization experiments.* BDS experiments in the presence of Dowex®

182   Optipore SD-2 resin were carried out in 250 mL shake flasks containing 20 mL of a 15.5 g

183   DCW/L resting cell suspension mixed with 20 mL of hexadecane containing 10000 µM DBT.

184   The resin was added to the mixture at resin concentrations of $X_r = 0$, 10 or 50 g/L in the shake

185   flask and the flasks were incubated at 30°C for 26 hours. After the 26-hour incubation period,

186   the mixtures were centrifuged for 15 min at 5000 RPM and the four components (oil, water, cells

187   and resin) were separated. DBT and HBP concentrations in the oil and aqueous components

188   were measured directly after centrifugation. DBT and HBP concentrations in the cells and resin

189   were measured by extraction into ethanol. Ethanol was selected as the best extractant among a

190   variety of solvents tested, including acetone, methanol, hexane, hexadecane, squalane, and

191   toluene. Cell wall solubilization by treatment with an enzymatic mixture of lysozyme (100

192   mg/mL) and mutanolysin (5000 Units/mL) did not increase the concentration of DBT or HBP

193   extracted from the cells. Sonication of the cells also did not increase extraction concentrations.

194   Loadings of HBP on the biocatalyst (L_c) and resin (L_r) were calculated from the expressions:

195 $$L_c = \frac{\left(\sum_i C_{extract,i}\right)V_{extract}}{m_{cells}}$$ (3)

196 $$L_r = \frac{\left(\sum_i C_{extract,i}\right)V_{extract}}{m_{resin}} ,$$ (4)

197 where $C_{extract,i}$ is the concentration of HBP in the *ith* extract, $V_{extract}$ is the volume of the extract

198 (constant for each fraction), m_{cells} is the mass of cells extracted, and m_{resin} is the mass of resin

199 extracted.

200

201 *DNA manipulations and preparation of E. coli recombinant strains.* Molecular biology

202 manipulations were performed according to standard protocols. Genomic DNA was extracted

203 from *R. erythropolis* IGTS8 using Promega's Wizard® genomic DNA purification kit. Each of

204 the desulfurization genes was PCR-amplified from the extracted genomic DNA with appropriate

205 primers (see Supplemental Material). Restriction sites for EcoRI and HindIII were included in

206 the primers. PCR amplicons were then cut with the appropriate restriction enzymes and ligated

207 with the pET-Duet vector that had been previously cut with the corresponding restriction

208 enzymes. The resulting vectors containing the four genes (*dszA, dszB, dszC* and *dszD*) were

209 sequence-verified. Each of the 4 vectors was then used to transform *E. coli* DH10B by

210 electroporation using 1 mm pathlength cuvettes. *E. coli* BL21 Star™ (DE3) One Shot® was

211 used as the expression host for each of the four desulfurization proteins, and transformed

212 according to the manufacturer's protocol (Invitrogen). Ampicillin selection (100 µg/mL) was

213 used to identify successful transformants.

214

215   *Protein expression and purification protocol.* The following protocol was followed to express

216   and purify each of the four desulfurization enzymes:

217   1.   A transformed *E. coli* BL21 colony from an LB-ampicillin plate was picked and grown in

218   10 mL LB with ampicillin at 30°C overnight.

219   2.   The next day, 1 L of LB medium with ampicillin was inoculated with 10 mL of overnight

220   culture and grown at 30°C with shaking at 250 RPM.

221   3.   The 1L culture was induced with 0.3 mM IPTG when the OD_{600} of the culture was 0.5-0.6.

222   Growth was continued for 18 hours at 20°C.

223   4.   Cells were harvested by centrifugation at 5000 RPM for 15 minutes at 4°C.

224   5.   The supernatant was discarded and the cell pellet was frozen at -20°C overnight.

225   6.   From this point on all cells and protein samples were maintained at 4°C or on ice to avoid

226   protein degradation. The cell pellet was resuspended using a volume of the 1X His buffer

227   (with 10% glycerol) equal to at least 2.5 times the mass of the cell pellet. Lysozyme (1

228   mg/mL) and DNAseI (500 µg/mL) were added and the cell suspension was incubated for

229   30 minutes on ice.

230   7.   The cell suspension was sonicated for 15-30 minutes at 90-100% amplitude with 1-second

231   on/1-second off cycle.

232   8.   Cell debris was pelleted by centrifugation at 20,000 rpm for 30 minutes at 4°C.

233   9.   The supernatant (20-40 mL) was mixed with 5 mL Ni-NTA agarose (Qiagen) in order to

234   bind the histidine-tagged desulfurization protein to the resin. The time for this binding step

235   was 1 hour at 4°C.

236   10.   After the 1 hour binding step, the protein-resin mixture was poured onto a Pierce®

237   centrifuge column (10 mL total volume) and the resin was allowed to settle. The flow-

238   through was processed by gravity flow and collected.

239   11.   The resin was washed with 10 mL of 1X His buffer containing 7.5 mM imidazole and the

240   flow through was collected. Then, the resin was treated with five different solutions of 1X

241   His buffer containing increasing imidazole concentrations of: 40, 60, 100, 250 and 500 mM

242   imidazole. Each solution was 5 mL in volume. The eluent of each fraction was collected.

243   12.   A diagnostic SDS-PAGE gel was run to determine the fractions with the highest purity.

244   These fractions were combined in one piece of snakeskin dialysis tubing and the protein

245   sample was dialyzed overnight in 1L of 50 mM Tris-HCl/50 mM NaCl/10% glycerol

246   buffer in the cold room with mild stirring.

247   13.   Finally, the dialyzed protein was flash-frozen using liquid nitrogen in small aliquots for

248   long-term storage at -80°C.

249

250   *Enzyme assays.*

251   All enzyme assays were performed in 20 mM phosphate buffer at pH 7.0 and 30°C. The assay

252   volume was 1000 μL for all assays. DszD assays were performed in semi-micro cuvettes and

253   maintained at room temperature. DszA, DszB and DszC assays were performed in 1.7 mL

254   Eppendorf tubes in a rotary shaker incubator at 30°C and 250 RPM and were quenched either by

255   addition of 1% of a 12 M HCl solution or by using an Amicon Ultra-0.5 mL 10 kDa spin filter

256   device to remove the enzyme. For DszD enzyme assays, either the concentration of NADH was

257   varied from 0-400 μM (at fixed FMN = 100 μM) or the concentration of FMN was varied from

258   0-100 μM (at fixed NADH = 150 μM), the concentration of DszD enzyme was 1.2 μg/mL, and

259   the assays were run for 10 minutes. For DszC enzyme assays, the concentration of NADH was

260   500 μM, FMN concentration was 10 μM, DBT concentration was varied from 0-5 μM, DszD

261   concentration was 0.47 μg/mL, DszC concentration was 3.1 μg/mL and the assays were run for 5

262   minutes. Assay conditions were identical for determining the mechanism of DszC inhibition by

263   HBPS and HBP except for the addition of those compounds at concentrations of 0-200 and 0-

264   1000 μM, respectively. For DszA enzyme assays, the NADH concentration was 500 μM, FMN

265   concentration was 10 μM, $DBTO_2$ was varied from 0-80 μM, DszD concentration was 1.4

266   μg/mL, DszA concentration was 6.7 μg/mL, and the assays were run for 3 min. For DszB

267   enzyme assays, the HBPS concentration was varied from 0-200 μM, DszB concentration was 3.5

268   μg/mL, and the assays were run for 5 min. For all four enzymes dose-response type assays were

269   performed to measure the inhibitory concentration leading to 50% reduction in enzyme activity

270   (IC_{50}). For DszD dose-response assays, the concentration of NADH was 500 μM and that of

271   FMN was 200 μM, the concentration of the various pathway intermediates was varied (DBT: 0-5

272   μM, $DBTO_2$: 0-80 μM, HBPS: 0-2000 μM, HBP: 0-2000 μM), the concentration of DszD was

273   4.7 μg/mL, and the assays were run for up to 5 minutes. For DszC dose-response assays, NADH

274   concentration was 500 μM, FMN concentration was 10 μM, DBT concentration was 5 μM, DszD

275   concentration was 0.47 μg/mL, DszC concentration was 0.3 mg/mL, the concentration of the

276   pathway intermediates was varied ($DBTO_2$: 0-80 μM, HBPS: 0-1000 μM, HBP: 0-2000 μM),

277   and the assays were run for 10 min. For DszA dose-response assays, the NADH concentration

278   was 500 μM, FMN concentration was 10 μM, $DBTO_2$ concentration was 80 μM, DszD

279   concentration was 1.4 μg/mL, DszA concentration was 67 μg/mL, the concentration of the

280   pathway intermediates was varied (DBT: 0-5 μM, HBPS: 0-500 uM, HBP: 0-1000 μM), and the

13

281   run time was 3 min. For DszB dose-response assays, HBPS concentration was 200 μM, the DszB

282   concentration was 58.5 μg/mL, the concentration of the pathway intermediates was varied (DBT:

283   0-5 μM, DBTO$_2$: 0-80 μM, HBP: 0-1000 μM), and the assays were run for 5 min.

284

285   *Analytical methods.* For DszD assays, the absorbance at 340 nm was measured using a

286   spectrophotometer to calculate the NADH concentration and this was used to calculate the

287   activity. The concentrations of DBT, DBTO$_2$, HBPS and HBP were measured using reversed

288   phase HPLC with a Zorbax SB-C18 column at a flow rate of 1 mL/min. For DszC and DszB

289   assays, the mobile phase was 50% acetonitrile-50% water and the temperature of the column was

290   maintained at 65°C. For DszA assays, the mobile phase was 30% acetonitrile-70% 10 mM

291   tetrabutylammonium bisulfate, 15 mM acetic acid pH 5.0 mobile phase and the temperature of

292   the column was maintained at 45°C.

293

294   **Results**

295   *Screening HBP-selective adsorbent resins.* A variety of commercially available resins were

296   screened for their ability to uptake HBP and DBT from a 0.50 vol/vol hexadecane-water solution

297   with an initial concentration of 10000 μM DBT and 10000 μM HBP in hexadecane. The resins

298   screened in this study were chosen because they span a wide range of resin hydrophobicity and

299   ionic functionalities, and most have been previously investigated in our lab (15). We found that

300   poly(styrene-*co*-DVB) derived resins generally have the greatest affinity for HBP (Figure 2A, *X$_r$*

301   = 10 g-resin/L-total for each resin). For instance, Dowex® Optipore L-493 and SD-2 were able

302   to achieve specific loadings of HBP of 40 and 50 mg/g-resin, respectively. In addition to having

303   the highest affinity for HBP of all the resins tested, Dowex® Optipore L-493 and SD-2 also

304   possessed the highest selectivity for HBP relative to DBT with HBP loadings that were 2.1 and

305   2.5 times greater than their respective DBT loadings. These resins were also found to have the

306   highest affinity for butanol, with specific loadings of butanol of 175 and 150 mg/g-resin,

307   respectively (15). The high affinity of these resins for butanol has been attributed to strong

308   hydrophobic interactions between the resin's π-π bonds of the aromatic side groups and the alkyl

309   chain of butanol and to the resin's high specific surface area (15). The affinity of these resins for

310   HBP is likely due to strong hydrophobic interactions between the resin's aromatic side groups

311   and the biphenyl part of HBP, though the specific loadings are reduced relative to n-butanol.

312

313   *Four-component BDS experiments.* We previously reported that the DBT desulfurization

314   activity of *R. erythropolis* IGTS8 was significantly reduced as HBP accumulated in the medium

315   during the BDS process (A. Abin-Fuentes, J.C. Leung, M.E.S Mohamed, D.I.C Wang, K.L.J.

316   Prather, submitted for publication). In particular, we found that the activity of a resting cell

317   suspension of 15.5 g DCW/L was decreased by 90% when the HBP concentration in the aqueous

318   medium reached 40 μM (A. Abin-Fuentes, J.C. Leung, M.E.S Mohamed, D.I.C Wang, K.L.J.

319   Prather, submitted for publication). In previous work, the use of Dowex® Optipore SD-2 in

320   butanol fermentations led to a decrease in aqueous phase concentration and increase in

321   productivity (15). In the current work, this resin, which had the best affinity and selectivity for

322   HBP of all resins studied, was used to try to mitigate the reduction in biocatalyst activity

323   correlated with HBP accumulation during the BDS process, thereby increasing the conversion of

324   DBT. *R. erythropolis* IGTS8 resting cell suspensions of 15.5 g DCW/L were mixed with

325   hexadecane (0.50 vol/vol) containing 10000 μM DBT and Dowex® Optipore SD-2 was added at

326   X_r of 0, 10 or 50 g/L. The four-component (oil, water, cells and resin) mixtures were incubated

327   at 30°C in a rotary shaker at 250 RPM for 26 hours. The concentration of DBT and HBP in each

328   component was measured at the end of the incubation period. The partition coefficient of HBP

329   between one component (component 1) and another component (component 2) in the four-

330   component BDS experiments is expressed as:

331    $$P_{comp1/comp2} = \frac{C_{HBP,comp1}}{C_{HBP,comp2}}, \tag{5}$$

332   where $C_{HBP,comp1}$ is the measured HBP concentration in component 1 and $C_{HBP,comp2}$ is the

333   measured HBP concentration in component 2. For example, $P_{R/C}$ is the partition coefficient of

334   HBP between the resin and the biocatalyst (cells). Similarly, $P_{O/W}$ is the partition coefficient of

335   HBP between hexadecane (oil) and water. The partition coefficients calculated at the different

336   resin concentrations are shown in Table I. The resin Dowex Optipore® SD-2 had the highest

337   affinity for HBP relative to the other components of the system. This resin had log $P_{R/C}$ and log

338    $P_{R/O}$ values around 2, which means that the resin's affinity for HBP was around 100 times greater

339   than the affinity of either the hexadecane oil phase or the biocatalyst. Furthermore, this resin had

340   a log $P_{R/W}$ around 4, which means that its affinity for HBP was around 10,000 times greater than

341   that of the aqueous buffer. The partition coefficients of HBP between oil and the aqueous buffer

342   ($P_{O/W}$) and between the biocatalyst and the aqueous buffer ($P_{C/W}$) were very similar (Table I).

343   The log $P_{O/W}$ and log $P_{C/W}$ in the absence of resin were 1.7 and 1.8, respectively. Also, the

344   partition coefficient of HBP between the biocatalyst and oil ($P_{C/O}$) was calculated to be 1 in the

345   absence of resin. The finding that $P_{O/W} \approx P_{C/W}$ and $P_{C/O} \approx 1$ indicates that the oil and biocatalyst

346   components have very similar affinity for HBP. Both the oil and the biocatalyst have an affinity

347   for HBP that is 50-60 times greater than that of the aqueous buffer in the absence of resin (Table

348   I).

349   The partition coefficient $P_{C/W}$ is defined as:

16

350 $$P_{C/W} = \frac{C_{HBP,\,intracellular}}{C_{HBP,\,water}}$$ (6)

351 where $C_{HBP,water}$ is the HBP concentration in the water phase and $C_{HBP,intracellular}$ is the HBP

352 concentration within the biocatalyst. The cell can be viewed as being composed of two

353 components: the inner cytoplasmic space and the outer envelope/shell that encompasses the

354 cytoplasm, which is the cell wall. The partition coefficient of HBP between the cytoplasm and

355 water ($P_{cytoplasm/W}$) was estimated from solving for its value in the expression:

356 $$P_{C/W} = P_{cell\,wall/W} f_{cell\,wall} + P_{cytoplasm/W} f_{cytoplasm}$$ (7)

357 where $P_{cell\,wall/W}$ is the partition coefficient of HBP between the cell wall and the water. The

358 value of $P_{cell\,wall/W}$ was estimated to be 550 (see Supplemental Material). $f_{cell\,wall}$ and $f_{cytoplasm}$ are

359 the fractions of the total volume of a single cell that are occupied by the cell wall and cytoplasm,

360 respectively. The values of $f_{cytoplasm}$ and $f_{cell\,wall}$ were calculated from the expressions:

361 $$f_{cytoplasm} = \frac{(R_{cell} - W)^3}{(R_{cell})^3}$$ (8)

362
363

364 $$f_{cell\,wall} = 1 - \frac{(R_{cell} - W)^3}{(R_{cell})^3},$$ (9)

365
366

367 where W is the thickness of the cell wall, which has been estimated to be approximately 10 nm

368 for *Rhodococcous* species (16). R_{cell} is the radius of the cell, which was estimated to be 0.5 μm

369 (17). The cytoplasmic HBP concentration ($C_{HBP,cytoplasm}$) was calculated from the following

370 expression:

371 $$C_{HBP,\,cytoplasm} = P_{cytoplasm/W}\, C_{HBP,water}$$ (10)

372   The value of $C_{HBP,cytoplasm}$ was calculated to be 1100, 330 and 260 μM at resin concentrations (X_r)

373   of 0, 10 and 50 g/L, respectively (Figure 2B). The corresponding HBP loadings on the

374   biocatalyst (L_c) were calculated to be 1.6, 0.5 and 0.2 mg HBP/g DCW using equation 3 (Figure

375   2B). These values show that the resin was effective in reducing HBP retention within the

376   cytoplasm of the biocatalyst, which is where the desulfurization enzymes are present (4).

377   Despite the significant decrease in HBP retained within the cytoplasm, the total amount of HBP

378   produced in the system did not increase with increasing resin concentration (Figure 2B).

379   Therefore, it was postulated that the biocatalyst, and in particular the desulfurization enzymes,

380   might be susceptible to cytoplasmic HBP concentrations smaller than 260 μM.

381

382   *Enzyme kinetics.* To study the kinetics of each enzyme, recombinant protein was expressed in

383   and purified from *E. coli* (See Supplemental Material). For DszA, DszB and DszD, the kinetic

384   data obtained was appropriately modeled by the Michaelis-Menten model (Figure 3A, 3B, 3D).

385   The equation for this model is:

386    $$v = \frac{k_{cat}[E_0][S]}{K_m + [S]} = \frac{V_{max}[S]}{K_m + [S]},$$ (11)

387   where v is the enzyme activity, k_{cat} is the turnover number, $[E_0]$ is the enzyme concentration in

388   each assay, $[S]$ is the substrate concentration and K_m is the Michaelis constant. The kinetics of

389   DszC could not be modeled accurately with a simple Michaelis-Menten model because it was

390   found that DszC was inhibited by its substrate DBT (Figure 3C). As a result, a substrate

391   inhibition model was used to fit the data obtained with DszC (18):

392    $$v = \frac{V_{max}[S]}{K_m + [S] + \dfrac{[S]^2}{K_{SI}}},$$ (12)

393   where K_{SI} is the substrate (DBT) inhibition constant.

394   The fitting of the models to the data was done using the *enzkin* package in MATLAB®. The

395   kinetic data obtained for all four desulfurization enzymes is shown in Figure 3. The kinetic

396   parameters of each enzyme are summarized in Table II and compared to parameters from other

397   studies, where available. To our knowledge, the only prior detailed characterization of a

398   desulfurization enzyme from *R. erythropolis* IGTS8 found $k_{cat} = 1.3 \pm 0.07$ min^{-1} and $K_m = 0.90$

399   ± 0.15 μM for DszB (6). In the current work, kinetic characterization of DszB yielded $k_{cat} = 1.7$

400   ± 0.2 min^{-1} and $K_m = 1.3 \pm 0.3$ μM, which are in good agreement with values from the previous

401   study. Rough preliminary characterization of DszA and DszD from *R. erythropolis* IGTS8

402   yielded k_{cat} values of "about 60 min^{-1}" and approximately 300 min^{-1}, respectively (4). The

403   corresponding values of k_{cat} for DszA and DszD measured in this work were 11 ± 2 min^{-1} and

404   760 ± 10 min^{-1}, which are of the same order of magnitude as those rough estimates from

405   preliminary characterization studies. DszC was inhibited by its substrate DBT and the kinetic

406   parameters obtained were $k_{cat} = 1.6 \pm 0.3$ min^{-1}, $K_m = 1.4 \pm 0.3$ μM and $K_{SI} = 1.8 \pm 0.2$ μM. The

407   activity of DszC from *R. erythropolis* D-1 was reported as 30.3 nmole $DBTO_2$/mg DszC/min

408   (19), which is in close agreement with the maximum activity measured in this work of 31.3

409   nmole $DBTO_2$/mg DszC/min (Figure 3C).

410   The catalytic efficiency of an enzyme is best defined by the ratio of the kinetic constants,

411   k_{cat}/K_m (20). The catalytic efficiency of each desulfurization enzyme was calculated (Table II).

412   The catalytic efficiencies of DszA, DszB, DszC were calculated to be 3.1, 1.3, 1.1 μM^{-1}min^{-1},

413   respectively. The catalytic efficiency of DszD on NADH and FMN was calculated to be 6.7 and

414   100 μM^{-1}min^{-1}, respectively. Therefore, the enzymes can be listed in order of decreasing

415   efficiency as: DszD > DszA > DszB ≈ DszC.

416

417 *Identification of four major inhibitory interactions in the 4S pathway.* All of the possible

418 interactions among the 4 different desulfurization enzymes and the four compounds in the

419 pathway (DBT, $DBTO_2$, HBPS and HBP) were studied to determine the major inhibitory

420 interactions. DBTO was not included because it is not typically observed during the BDS

421 process because its rate of consumption is much faster than its rate of generation (4). The

422 strength of inhibition was studied by means of a dose-response plot. The dose-response equation

423 describing the effect of inhibitor concentration on enzyme activity is expressed as (20):

424 $$\frac{v_i}{v_0} = \frac{1}{1 + \frac{[I]}{IC_{50}}},$$ (13)

425 where v_i is the enzyme's activity at an inhibitor concentration of [I], v_0 is the enzyme's activity in

426 the absence of inhibitor, and IC_{50} is the concentration of inhibitor required to reduce the

427 enzyme's activity by 50%. The IC_{50} parameter is phenomenological and has no mechanistic

428 implications. The value of IC_{50} was obtained by fitting the data of v_i /v_0 versus [I] using the non-

429 linear fitting package *nlinfit* in MATLAB® to the dose-response equation. The four major

430 inhibitory interactions identified were (in order of decreasing strength): DszC inhibition by

431 HBPS ($IC_{50} = 15 \pm 2$ μM), DszC inhibition by HBP ($IC_{50} = 50 \pm 5$ μM), DszA inhibition by HBP

432 ($IC_{50} = 60 \pm 5$ μM) and DszB inhibition by HBP ($IC_{50} = 110 \pm 10$ μM) (Figure 4 and Table III).

433 Note that the IC_{50} values of all four inhibitory interactions are significantly smaller than the

434 estimated cytoplasmic HBP concentration. Even in the best-case scenario, when 50 g/L of a

435 highly HBP-selective resin was added to the BDS mixture, the estimated cytoplasmic HBP

436 concentration was still 260 μM. This finding suggests that these four inhibitory interactions are

437   likely responsible for the reduction in biocatalyst activity that is observed during a typical BDS

438   process when HBP is generated endogenously from DBT within the biocatalyst.

439   The only prior preliminary characterization of inhibition within the 4S pathway showed

440   that DszB from *R. erythropolis* KA2-5-1 had an IC_{50} of around 2000 μM with respect to HBP

441   (12). We report here three new inhibitory interactions in the pathway that are stronger than any

442   previous preliminary findings. Note that the strongest inhibitory interactions are on the first

443   enzyme in the pathway, DszC, and the strength of inhibition decreases farther down the pathway,

444   with the last enzyme in the pathway, DszB, having the weakest HBP inhibition at $IC_{50} = 110$ μM

445   (Figure 4B). Note also that the major inhibitory compounds in the pathway are the last two

446   intermediates, HBPS and HBP. This pattern of inhibition is typical of feedback inhibition of

447   linear pathways; for example, in the tricarboxylic acid (TCA) cycle the first enzyme in the

448   pathway is strongly inhibited by the end product ATP.

449   *Mechanism of the major inhibitory interactions in the 4S pathway.* The telltale sign of non-

450   competitive inhibition is a reduced V_{max} without a change in K_m as the inhibitor concentration is

451   increased (20). This phenomenon was observed in the inhibition of DszC by both HBPS and

452   HBP (Figure 5A and Figure 5B). The model for non-competitive inhibition of an enzyme that

453   obeys Michaelis-Menten kinetics is given by (20):

454     $$v = \frac{V_{max}[S]}{K_m\left(1+\dfrac{[I]}{K_I}\right)+[S]\left(1+\dfrac{[I]}{\alpha K_I}\right)},$$ (14)

455   where [I] is the inhbitior concentration, K_i is the inhibition constant, and α is a parameter that

456   reflects the effect of inhibitor on the affinity of the enzyme for its substrate, and likewise the

457 effect of the substrate on the affinity of the enzyme for the inhibitor. Non-competitive inhibition

458 refers to the case in which an inhibitor displays binding affinity for both the free enzyme and the

459 enzyme-substrate binary complex (see Supplemental Material). This form of inhibition is the

460 most general case; in fact, competitive and uncompetitive inhibition can be viewed as special,

461 restricted cases of non-competitive inhibition in which the value of α is infinity or zero,

462 respectively (20). Since the kinetics of DszC showed substrate inhibition, a modification to the

463 non-competitive model was derived (see Supplemental Material). The non-competitive

464 inhibition of DszC by HBPS and HBP can be expressed as:

465
$$v = \frac{V_{max}[S]}{K_m\left(1+\dfrac{[I]}{K_I}\right)+[S]\left(1+\dfrac{[I]}{\alpha K_I}\right)+\dfrac{[S]^2}{K_{SI}}}$$
(15)

466 The solid lines in Figures 5A and 5B represent the fits for the non-competitive inhibition model

467 (equation 15), where the values of K_i and α were 13.5 μM and 0.13 for HBPS inhibition and 40

468 μM and 0.4 for HBP. Fitting of the model to the data was attempted using *nlinfit* from

469 MATLAB®, but was unsuccessful due to convergence issues. Instead the parameters were

470 determined by a graphical method outlined in section 8.3 of (20). The first step in this method

471 was the construction of the double-reciprocal Lineweaver-Burk plot. To obain the values of K_i

472 and αK_i two secondary plots were constructed. The first of these was a Dixon plot of $1/V_{max}$ as a

473 function of [I], from which the value of $-\alpha K_i$ can be determined as the x-intercept. In the second

474 plot, the slopes of the double-reciprocal lines (from the Lineweaver-Burk plot) are plotted as a

475 function of [I]. For this plot, the x-intercept will be equal to $-K_i$. Combining the information

476 from these two secondary plots allows determination of both inhibition parameters. The

22

477   mechanism of DszB inhibition by HBP and DszA inhibition by HBPS could not be determined

478   due to limited resolution of the HPLC detector.

479

480   *Enzyme inhibition model predicts reduction in biocatalyst activity.* A model that

481   incorporated enzyme inhibition was developed to predict the volumetric desulfurization rate in

482   biphasic (oil-water) BDS experiments (See Supplemental Material for model equations). The

483   model accounted for DBT and HBP in three components: oil, water and cytoplasm. The two

484   pathway intermediates, $DBTO_2$ and HBPS, were assumed to only be present in the cytoplasm.

485   The three major inhibitory interactions by HBP on DszA, DszB and DszC were taken into

486   account. The fourth major inhibitory interaction, the inhibition of DszC by HBPS, was ignored

487   for simplicity. DszD activity was assumed to not be limiting and was therefore excluded from

488   the model. Loss of biocatalyst activity unrelated to HBP accumulation was also taken into

489   account in the model through an exponential decay constant, k_d (See Supplemental Material).

490   Concentrations of DszA, DszB and DszC were assumed to be all the same and equal to E_0. E_0

491   was the only floating parameter in the model. The value of E_0 was obtained by allowing its value

492   to vary until the initial desulfurization rate predicted by the model matched the measured

493   desulfurization rate. The value of E_0 obtained was 15 mg/mL, so that the total concentration of

494   desulfurization enzymes in the cytoplasm was 45 mg/mL. This value is of the same order as the

495   total cytoplasmic concentration of protein, which has been reported to be approximately 200

496   mg/mL (22).

497   The first step in the biphasic BDS experiments was growth of biocatalyst in a 4L

498   bioreactor to a cell density of 29-35 g DCW/L. Next, 10 % vol/vol hexadecane containing

499   100,000 μM DBT was added to the bioreactor. The desulfurization rate of DBT in the bioreactor

500   was monitored thereafter from the measured concentrations of DBT and HBP in the hexadecane

501   and aqueous phases. For the first two hours after hexadecane addition, the mixing speed was

502   maintained at 200 RPM. The mixing speed was increased to 500 RPM thereafter to minimize

503   mass transport limitations in the system. The enzyme inhibition model was used to predict the

504   desulfurization rate only after the shift in mixing speed to 500 RPM. The model predicts the

505   concentration of HBP in the oil and water phase and the volumetric desulfurization rate

506   accurately (Figures 6A, 6B and 6C). The coefficient of determination (R^2) between the model

507   and the data was calculated to be 0.96 using the MATLAB® function *corr(X,Y)*.

508

509   **Discussion**

510   Dose-response experiments were performed to investigate the potential inhibitory effect of the

511   various intermediates in the 4S pathway on the desulfurization enzymes. Four major inhibitory

512   interactions were identified, all of which had IC_{50} values under 110 μM. Three of the four major

513   inhibitory interactions were carried out by HBP. HBP was found to inhibit DszA, DszB and

514   DszC with IC_{50} values of 60, 110 and 50 uM, respectively. The fourth major inhibitory

515   interaction identified is the inhibition of DszC monooxygenase by HBPS. This interaction is the

516   strongest of the four since it has the lowest IC_{50} value of 15 μM. HBPS concentration during the

517   four-component BDS experiments was not measured in this work. The IC_{50} values of HBP on

518   the desulfurization enzymes are all significantly lower than the minimum cytoplasmic HBP

519   concentration estimated during the four-component BDS experiments, which was 260 μM. This

520   suggests that enzyme inhibition by HBP was responsible for the reduction in biocatalyst activity

521   during the four-component BDS experiments, even in the presence of 50 g/L of HBP-selective

522   resin (Dowex ® Optipore SD-2). In the n-butanol fermentation by *Clostridium acetobutylicum*

24

523 ATCC 824, n-butanol productivity was increased two-fold upon addition of Dowex® Optipore

524 SD-2 to the medium (15). However, the n-butanol toxicity threshold of *Clostridium* is generally

525 considered to be about 1.3% (wt./vol.), which is approximately 180 mM (15). The fact that the

526 inhibitory levels of HBP on the *R. erythropolis* IGTS8 desulfurization enzymes are at least 3

527 orders of magnitude smaller than the toxicity levels of n-butanol on *Clostridium* might explain

528 why n-butanol productivity by *Clostridium* was enhanced upon addition of Dowex ® Optipore

529 SD-2 while HBP productivity by *R.erythropolis* IGTS8 was not enhanced.

530   In another study, *R. erythropolis* IGTS8 lysates were supplied with 200 μM DBT initially

531 and the concentrations of DBT, $DBTO_2$, HBPS and HBP were monitored over time (4). After 10

532 minutes, all DBT was depleted, the HBPS concentration was approximately 130 μM and the

533 HBP concentration was approximately 50 μM (4). From 10 to 60 minutes, the HBPS

534 concentration decreased steadily from 130 to 0 μM and the HBP concentration increased from 50

535 to 200 μM. No $DBTO_2$ was detected at any time (4). All of these results agree with the kinetic

536 data obtained in this work. First of all, since the k_{cat} of DszA is approximately 7 times that of

537 DszC (Table II), $DBTO_2$ consumption rate is expected to be significantly greater than its

538 generation rate, which agrees with the fact that no $DBTO_2$ was detected. Second, the buildup of

539 HBPS within the first 10 min is consistent with the fact that its consumption rate (DszB k_{cat} = 1.7

540 min^{-1}) is significantly slower than its generation rate (DszA k_{cat} = 11.2 min^{-1}) (Table II). The fact

541 that the HBP concentration accumulates to over 130 μM within the first few minutes indicates

542 that DszC would have been severely inhibited by HBPS at that point in time. As HBPS is

543 consumed, DszC inhibition by HBPS is relieved but then HBP inhibition of DszC (and DszA and

544 DszB) become more significant. Therefore, we expect that during a BDS experiment all four

545 major inhibitory interactions reported here would be important. HBPS inhibition of DszC is

546 responsible for maintaining the BDS rate low at the beginning of the BDS process when HBP

547 levels are still low. Once HBP levels rise, HBP inhibition of DszA, DszB and DszC will be

548 mostly responsible for inhibition of the BDS rate.

549   Due to the biocatalyst's high affinity for HBP relative to the aqueous buffer ($P_{C/W}$ = 60 at

550 X_r = 0 g/L), the intracellular HBP concentration ($C_{HBP,intracellular}$) is much higher than the HBP

551 concentration in the aqueous buffer ($C_{HBP,water}$). In previous studies, HBP inhibition in biphasic

552 (oil-water) BDS experiments has been downplayed due to the partition coefficient of HBP

553 between oil and water ($P_{O/W}$) being high (around 40-50) (23). It has been generally assumed that

554 since the biocatalyst resides in the aqueous phase, the intracellular concentration of HBP is

555 similar to the aqueous phase concentration. This assumption is in part because the biocatalyst's

556 affinity for HBP has not been quantified in previous studies. We have shown that this affinity

557 for HBP is in par with that of the oil phase. As a result, HBP retention within the biocatalyst and

558 HBP inhibition of the desulfurization enzymes is an obstacle even in biphasic BDS experiments.

559   The affinity of the biocatalyst for HBP is an intrinsic property of the biocatalyst and will

560 likely vary depending on the biocatalyst employed. Interactions between cyclic hydrocarbons

561 and biological membranes have been previously investigated (24). The partition coefficients of a

562 range of cyclic hydrocarbons (including aromatics) between liposomes prepared from *E. coli*

563 phospholipids and an aqueous phosphate buffer were measured. From these measured partition

564 coefficients, a correlation for predicting the partition coefficient of any cyclic hydrocarbon

565 between the liposome (membrane) and the aqueous buffer ($P_{M/B}$) based on the octanol-water

566 partition coefficient ($P_{O/W}$) of that cyclic hydrocarbon was developed. The liposome-buffer

567 partition coefficient of HBP is predicted to be $\log(P_{M/B})$ = 2.2 given the known value of the

568 octanol-water partition coefficient $\log(P_{O/W})$ = 3.09 (25). This is in good agreement with the

569   value of the partition coefficient of HBP between the biocatalyst and the buffer measured in this

570   work of $\log(P_{C/W}) = 1.8\text{-}2.2$ (Table I). The liposomes prepared by Sikkema et al (1994) are

571   representative of the cytoplasmic membrane of a gram-negative bacterium. *R. erythropolis*,

572   being a gram-positive bacteria, has a thin cytoplasmic membrane surrounded by a thick cell wall

573   made mostly of peptidoglycan sturcutre and mycolic acids (10). The fact that the value of

574    $\log(P_{C/W})$ measured in this study agrees well with the predicted value of $\log(P_{M/B})$ suggests that

575   HBP retained by *R. erythropolis* IGTS8 might reside mostly within the cytoplasmic membrane as

576   opposed to the cell wall, which is structurally very different. This idea agrees with the

577   mechanism of DBT to HBP conversion during the BDS process. When DBT is added

578   exogenously, it is transported into the cell (likely by passive diffusion). Inside the cytoplasm, the

579   DBT is transformed to HBP via the 4S pathway and then the HBP will interact first with the

580   cytoplasmic membrane as it attempts to exit the cell.

581

582   **Conclusions**

583   In this work, the mechanism of biocatalyst inhibition in the BDS of DBT was investigated.

584   Retention of the final product HBP during the BDS process to concentrations in the hundreds of

585   μM range or higher leads to inhibition of the three enzymes in the linear part of the 4S pathway.

586   These three enzymes DszA, DszB and DszC have IC_{50} values with respect to HBP of 60, 110

587   and 50 μM, respectively. Host engineering to reduce retention of HBP might mitigate inhibition

588   of the 4S pathway by HBP. This poses a formidable challenge as it has been suggested that the

589   cytoplasmic membrane, which is ubiquitous in nature, may be responsible for HBP retention

590   within the biocatalyst. Protein engineering might also be explored as a means to overcome

591   inhibition of the pathway enzymes.

592

Acknowledgements

Nomenclature

598 C_{HBP} – concentration of HBP (µM)

599 $[E_0]$ – total enzyme concentration

600 $f_{cytoplasm}$ – volume fraction of a single cell occupied by cytoplasm

601 $f_{cell\ wall}$ – volume fraction of a single cell occupied by cell wall

602 $[I]$ – Inhibitor concentration (µM)

603 IC_{50} – inhibitor concentration that reduces enzyme's activity by 50%

604 k_{cat} – enzyme turnover number (min^{-1})

605 K_m – Michaelis constant (µM)

606 K_{SI} – substrate inhibition constant (µM)

607 K_i – enzyme inhibition constant

608 L_c – loading of HBP on the cells (mg HBP/g DCW)

609 L_r – loading of HBP on resin (mg HBP/g resin)

610 m_c – mass of cells (g DCW)

611 m_r – mass of resin (g)

612 $P_{O/W}$ – HBP partition coefficient between hexadecane and aqueous buffer

613 $P_{C/W}$ – HBP partition coefficient between biocatalyst and aqueous buffer

614 $P_{R/W}$ – HBP partition coefficient between resin and aqueous buffer

615 $P_{C/O}$ – HBP partition coefficient between biocatalyst and hexadecane

616 $P_{R/C}$ – HBP partition coefficient between resin and biocatalyst

617 $P_{R/O}$ – HBP partition coefficient between resin and hexadecane

618 $P_{cell\ wall/W}$ – HBP partition coefficient between the cell wall and aqueous buffer

619 $P_{cytoplasm/W}$ – HBP partition coefficient between cytoplasm and aqueous buffer

620   R_{cell} – radius of the cell (μm)

621   [S] – Substrate concentration (μM)

622   V_{total} – total volume of oil, water and resin in HBP adsorption by resin experiments (L)

623   V_{max} – maximum enzyme activity (nmole product/g enzyme/min)

624   W – thickness of the cell wall (nm)

625   X_r – resin concentration (g/L)

626   α – parameter that reflects effect of inhibitor on enzyme's affinity for its substrate

627   v_0 – enzyme's activity in the absence of inhibitor (nmole product/g enzyme/min)

628

629

630   **References**

631   1.   Soleimani M, Bassi A, Margaritis A. 2007. Biodesulfurization of refractory organic

632   sulfur compounds in fossil fuels. Biotech. Adv. 25: 570-596.

633   2.   Kilbane JJ. 2006. Microbial biocatalyst developments to upgrade fossil fuels. Curr. Opin.

634   Biotechnol. 17:305–314

635   3.   Gray KA, Mrachko GT, Squires CH. 2003. Biodesulfurization of fossil fuels. Curr. Opin.

636   Microbiol. 6:229–235

637   4.   Gray KA, Pogrebinsky OS, Mrachko GT, Xi L, Monticello DJ, Squires CH. 1996.

638   Molecular mechanisms of biocatalytic desulfurization of fossil fuels. Nat. Biotech. 14:

639   1705-1709

640   5.   Xi L, Squires CH, Monticello DJ, Childs JD. 1997. A flavin reductase stimulates DszA

641   and DszC proteins of *Rhodococcus erythropolis* IGTS8 in vitro. Biochem. Biophys. Res.

642   Commun. 230:73-75

643   6.   Watkins LM, Rodriguez R, Schneider D, Broderick R, Cruz M, Chambers R, Ruckman

644   E, Cody M, Mrachko GT. 2003. Purification and characterization of the aromatic

645   desulfinase 2-(2'-hydroxyphenyl)benzenesulfinate desulfinase. Biochem. Biophys.

646   415:14-23

647   7.   Schilling BM, Alvarez LM, Wang DIC, Cooney CL. Continuous desulfurization of

648   dibenzothiophene with *R. rhodochrous* IGTS8 (ATCC 53968). Biotechnol. Prog.

649   18:1207–1213.

650   8.   Naito M, Kawamoto T, Fujino K, Kobayashi M, Maruhashi K, Tanaka A. 2001. Long-

651   term repeated desulfurization by immobilized *Rhodococcus erythropolis* KA2-5-1 cells.

652   Appl. Microbiol. Biotechnol. 55:374–378.

653   9.   Jia X, Wen J, Sun Z, Caiyin Q, Xie S. 2006. Modeling of DBT biodegradation behaviors

654   by resting cells of *Gordonia* sp.WQ-01 and its mutant in oil–water dispersions. Chem.

655   Eng. Sci. 61: 1987 – 2000

656   10. Lichtinger T, Reiss G, Benz R. 2000. Biochemical identification and biophysical

657   characterization of a channel-forming protein from *Rhodococcus erythropolis*. J.

658   Bacteriol. 182(3): 764-770.

659   11. Honda H, Sugiyama H, Saito I, Kobayashi T. 1998. High cell density culture of

660   Rhodococcus rhodochrous by pH-stat feeding and dibenzothiophene degradation. J.

661   Ferment. Bioeng. 85: 334 –338.

662   12. Nakayama N, Matsubara T, Ohshiro T, Moroto Y, Kawata Y, Koizumi K, Hirakawa Y,

663   Suzuki M, Maruhashi K, Izumi Y, Kurane R. 2002. A novel enzyme, 2′-

664   hydroxybiphenyl-2-sulfinate desulfinase (DszB), from a dibenzothiophene-desulfurizing

665   bacterium *Rhodococcus erythropolis* KA2-5-1: gene overexpression and enzyme

666   characterization. Biochim. Biophys. Acta 1598:122–130.

667   13. Caro A, Boltes K, Leton P, Garcia-Calvo E. 2008. Description of by-product inhibition

668   effects on biodesulfuriation of dibenzothiophene in biphasic media. Biodegradation 19:

669   599-611.

670   14. Chen H, Zhang WJ, Cai YB, Zhang Y, Li W. 2008. Elucidation of 2-hydroxybiphenyl

671   effect on dibenzothiophene desulfurization by Microbacterium sp. strain ZD-M2. Biores.

672   Tech. 99:6928-33.

673   15. Nielsen DR, Prather KJ. 2009. In situ product recovery of n-butanol using polymeric

674   resins. Biotechnol. Bioeng. 102(3): 811-821

675   16. Sutcliffe IC, Brown AK, Dover LG. 2010. The rhodococcal cell envelope: composition,

676   organization and biosynthesis. Biology of Rhodococcus. Microbiology Monographs 16.

677   Springer-Verlag Berlin Heidelberg.

678 17. Kilbane JJ. 1992. Mutant microorganisms useful for cleavage of organic C-S bonds. US

679   patent 5,104,801.

680 18. Shuler ML, Kargi F . 2002. Bioprocess Engineering: Basic concepts. Second Edition.

681   Prentice Hall, Inc.

682 19. Ohshiro T, Suzuki K, Izumi Y. 1997. Dibenzothiophene (DBT) degrading enzyme

683   responsible for the first step of DBT desulfurization by *Rhodococcus erythropolis* D-1:

684   Purification and characterization. J. Biosci. Bioeng. 83(3):233-237.

685 20. Copeland RA. 2000. Enzymes: a practical introduction to structure, mechanism, and

686   data analysis. Second edition. Wiley-VCH p. 397

687 21. Matsubara T, Ohshiro T, Nishina Y, Izumi Y. 2001. Purification, characterization, and

688   overexpression of flavin reductase involved in dibenzothiophene desulfurization by

689   *Rhodococcus erythropolis* D-1. Appl. Environ. Microbio. 67(3):1179-1184

690 22. Ellis RJ. 2001. Macromolecular crowding: obvious but underappreciated. Trends

691   Biochem. Sci. 26(10): 597-604

692 23. Caro A, Boltes K, Leton P, Garcia-Calvo E. 2007. Dibenzothiophene biodesulfurization

693   in resting cell conditions by aerobic bacteria. J. Biochem. Eng. 35(2): 191-197

694 24. Sikkema J, de Bont JAM, Poolman B. 1994. Interactions of cyclic hydrocarbons with

695   biological membranes. J. Bio. Chem. 269(11):8022-8028.

696 25. Hansch C, Leo A, Hoekman D. 1995. Exploring QSAR. Washington DC: American

697   Chemical Society. P. 97

698

699

Tables

Table I. Comparison of partition coefficients between the four different components in the four component BDS experiments in the presence of the resin Dowex® Optipore SD-2.

Resin concentration (g/L)	$P_{C/O}$	$P_{C/W}$	$P_{O/W}$	$P_{R/C}$	$P_{R/O}$	$P_{R/W}$
0	1	60	52	-	-	-
10	1	47	42	88	99	4116
50	3	160	54	99	296	15906
Resin concentration (g/L)	$\log P_{C/O}$	$\log P_{C/W}$	$\log P_{O/W}$	$\log P_{R/C}$	$\log P_{R/O}$	$\log P_{R/W}$
0	0.1	1.8	1.7	-	-	-
10	0.0	1.7	1.6	1.9	2.0	3.6
50	0.5	2.2	1.7	2.0	2.5	4.2

C – cells
O – oil
W – water
R – resin

Table II. Summary of the main properties of the Dsz enzymes purified in this work including the molecular weight (MW), stock concentration and measured kinetic constants.

Enzyme	M_w (kDa)	Stock Concentration (mg/mL)	This work			Other authors	
			k_{cat} (min^{-1})	K_m (μM)	k_{cat}/K_m (μM^{-1} min^{-1})	k_{cat} (min^{-1})	K_m (μM)
DszA	49.6	1.3	11±2	3.6 ± 0.5	3.1	"about 60"[a]	"approx. 1"[a]
DszB	39.0	1.2	1.7±0.2	1.3 ± 0.3	1.3	1.3 ± 0.07 [b]	0.90 ± 0.15 [b]
DszC	45.0	6.1	1.6±0.3	1.4 ± 0.3, K_{SI} = 3 ± 0.2 μM	1.1	n/a	"less than 5"[a]
DszD	25.0	4.7	760±10	114 ± 5 (NADH), 7.3 ± 0.5 (FMN)	6.7 (NADH), 100 (FMN)	~300 [c]	208 (NADH), 10.8 (FMN) [d]

[a] Strain used was *R. erythropolis* IGTS8 (4)
[b] Strain used was *R. erythropolis* IGTS8 (6)
[c] Calculated estimate based on data in (4). Strain used was *R. erythropolis* IGTS8
[d] Strain used was *R. erythropolis* D-1 (21)

Table III. Summary of inhibition parameters for the four major inhibitory interactions including the mechanism of inhibition, the K_I, α and IC_{50} values.

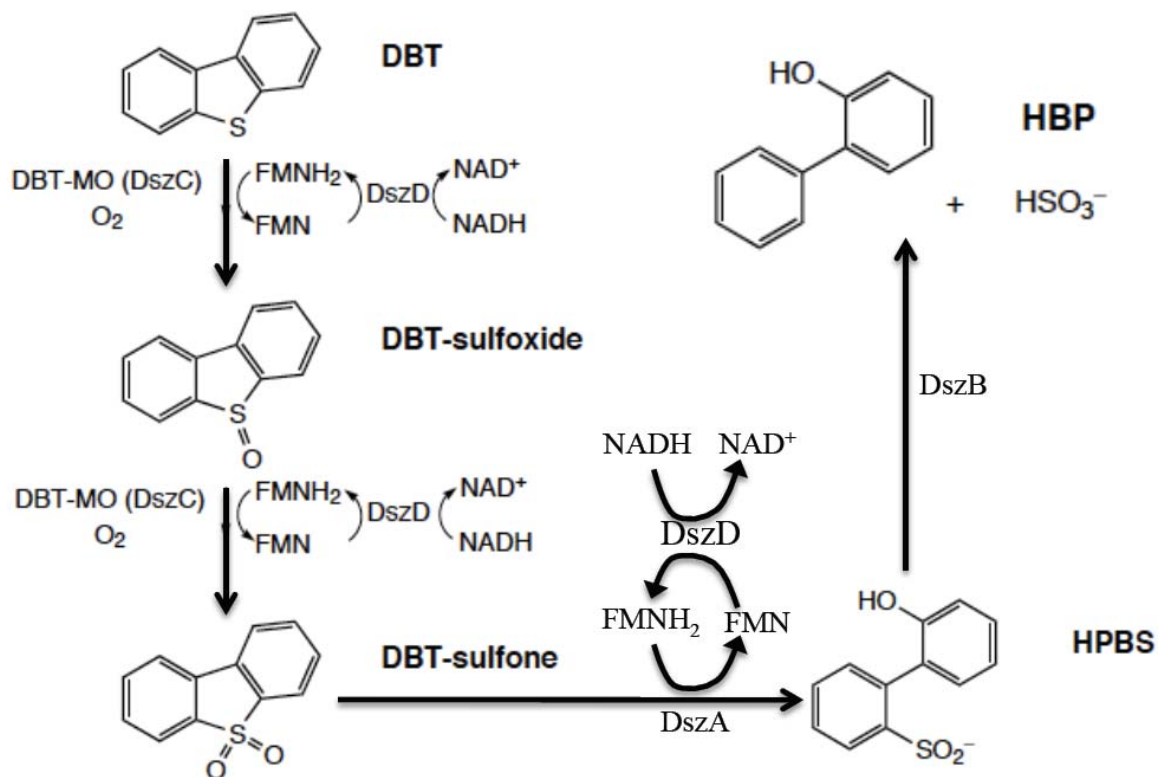| Enzyme	Inhibitor	Mechanism	K_I (μM)	α	IC_{50} (μM)
DszA	HBP	Not determined	n/a	n/a	60 ± 5
DszB	HBP	Not determined	n/a	n/a	110 ± 10
DszC	HBPS	Non-competitive	13.5	0.13	15 ± 2
DszC	HBP	Non-competitive	40	0.4	50 ± 5

Figure Captions

Figure 1. The four-step biodesulfurization 4S pathway. The first two steps, catalyzed by both

DszC and DszD, are the conversion of DBT to DBT-sulfoxide (DBTO) and then to DBT-sulfone

(DBTO$_2$). The third step, catalyzed by both DszA and DszD, is the conversion of DBTO$_2$ to

HBPS. The final step is the conversion of HBPS to HBP by DszB.

Figure 2. (A) – Specific loading of HBP (white) and DBT (black) by the various resins tested at

a resin concentration of 10 g/L from a 0.50 vol./vol. hexadecane-water solution containing 10

mM DBT and 10 mM HBP initially. (B) – Total HBP produced (white) and cytoplasmic HBP

concentration (black) in four-component BDS experiment at 15.5 g DCW/L, oil fraction 0.50

vol/vol and 10 mM DBT. Specific HBP loadings are shown above black columns. Data shown

are the average and standard deviations of 3 replicates.

Figure 3. Enzyme kinetics for DszA (A), DszB (B), DszC (C), and DszD (D). Diamonds

represent data and solid lines represent Michaelis-Menten model fits for DszA, DszB and DszD

and substrate inhibition model for DszC. Data shown are the average and standard deviations of

3 replicates.

Figure 4. Normalized desulfurization enzyme activity at different inhibitor concentrations for

the four major inhibitory interactions identified in the 4S pathway. (A) – DszA inhibition by

HBP has an IC$_{50}$ of 60 ± 5 μM; (B) – DszB inhibition by HBP has an IC$_{50}$ of 110 ± 10 μM; (C) –

DszC inhibition by HBPS has an IC$_{50}$ of 15 ± 2 μM; (D) – DszC inhibition by HBP has an IC$_{50}$

of 50 ± 5 μM. Data shown are the average and standard deviations of 3 replicates.

728

729 **Figure 5.** Non-competitive inhibition of DszC by HBPS and HBP. (A) – DszC activity at a

730 range of DBT substrate concentrations from 0-5 μM and HBPS concentrations of 0 μM (closed

731 diamonds), 5 μM (closed squares), 25 μM (closed triangles) and 50 μM (crosses). (B) – DszC

732 activity at a range of DBT substrate concentrations from 0-5 μM and HBP concentrations of 0

733 μM (closed diamonds), 100 μM (closed squares), 500 μM (closed triangles). Solid lines are

734 model fits from equation 15.

735

736 **Figure 6.** Enzyme inhibition model predictions for BDS bioreactor experiment. (A) –

737 Volumetric desulfurization rate data (circles) and model prediction (line). (B) – Concentration of

738 HBP in the oil phase data (circles) and model (line). (C) – Concentration of HBP in the water

739 phase data (circles) and model (line). Data shown are the average and standard deviations of 3

740 replicates.

741

Figures

Figure 1. The four-step biodesulfurization 4S pathway. The first two steps, catalyzed by both DszC and DszD, are the conversion of DBT to DBT-sulfoxide (DBTO) and then to DBT-sulfone (DBTO$_2$). The third step, catalyzed by both DszA and DszD, is the conversion of DBTO$_2$ to HBPS. The final step is the conversion of HBPS to HBP by DszB.
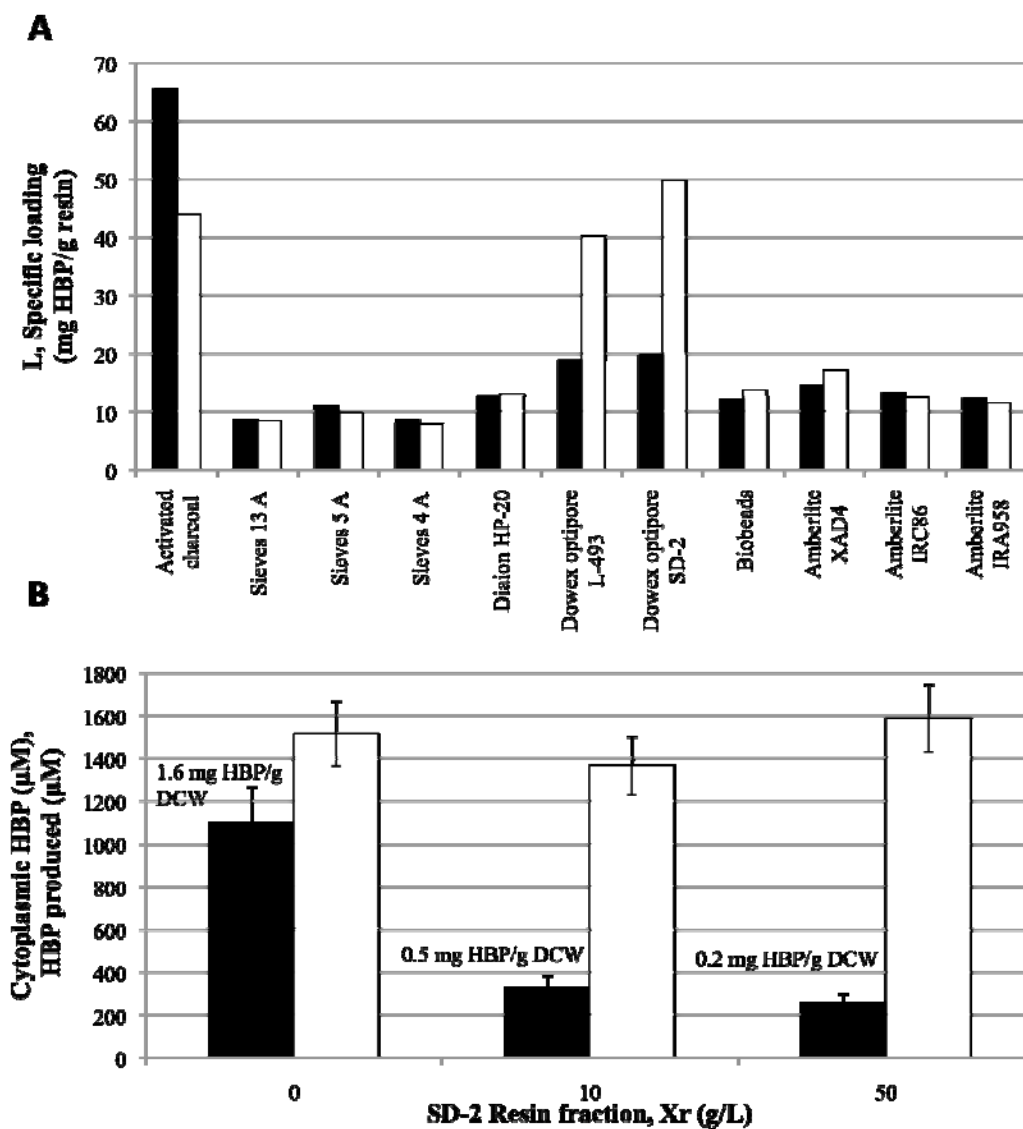
743

Figure 2. (A) – Specific loading of HBP (white) and DBT (black) by the various resins tested at a resin concentration of 10 g/L from a 0.50 vol./vol. hexadecane-water solution containing 10 mM DBT and 10 mM HBP initially. (B) – Total HBP produced (white) and cytoplasmic HBP concentration (black) in four-component BDS experiment at 15.5 g DCW/L, oil fraction 0.50 vol/vol and 10 mM DBT. Specific HBP loadings are shown above black columns. Data shown are the average and standard deviations of 3 replicates.

744

745

746

Figure 3. Enzyme kinetics for DszA (A), DszB (B), DszC (C), and DszD (D). Diamonds represent data and solid lines represent Michaelis-Menten model fits for DszA, DszB and DszD and substrate inhibition model for DszC. Data shown are the average and standard deviations of 3 replicates.

747

Figure 4. Normalized desulfurization enzyme activity at different inhibitor concentrations for the four major inhibitory interactions identified in the 4S pathway. (A) – DszA inhibition by HBP has an IC_{50} of 60 ± 5 μM; (B) – DszB inhibition by HBP has an IC_{50} of 110 ± 10 μM; (C) – DszC inhibition by HBPS has an IC_{50} of 15 ± 2 μM; (D) – DszC inhibition by HBP has an IC_{50} of 50 ± 5 μM. Data shown are the average and standard deviations of 3 replicates.

748

749

750

751

752

753

754

755

756
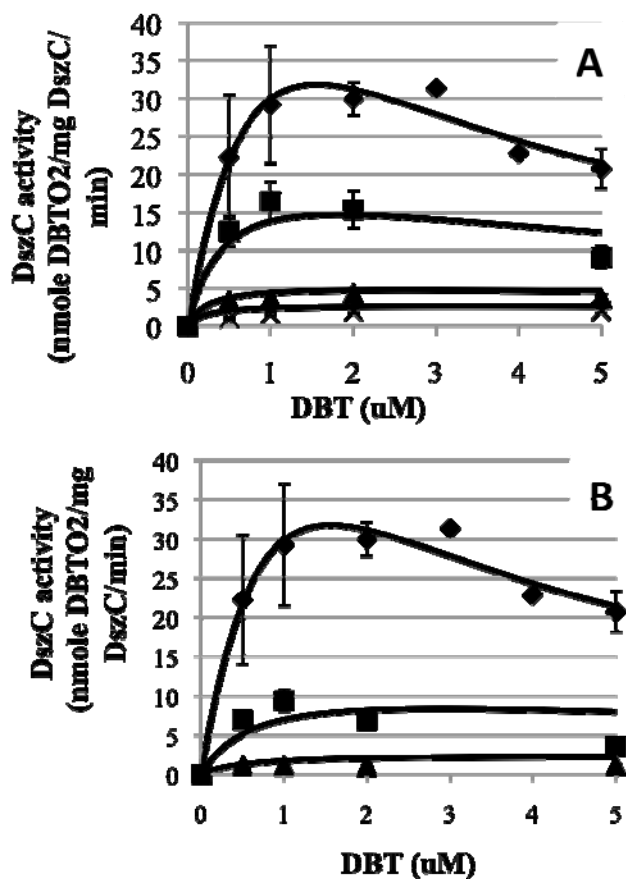
Figure 5. Non-competitive inhibition of DszC by HBPS and HBP. (A) – DszC activity at a range of DBT substrate concentrations from 0-5 μM and HBPS concentrations of 0 μM (closed diamonds), 5 μM (closed squares), 25 μM (closed triangles) and 50 μM (crosses). (B) – DszC activity at a range of DBT substrate concentrations from 0-5 μM and HBP concentrations of 0 μM (closed diamonds), 100 μM (closed squares), 500 μM (closed triangles). Solid lines are model fits from equation 15.
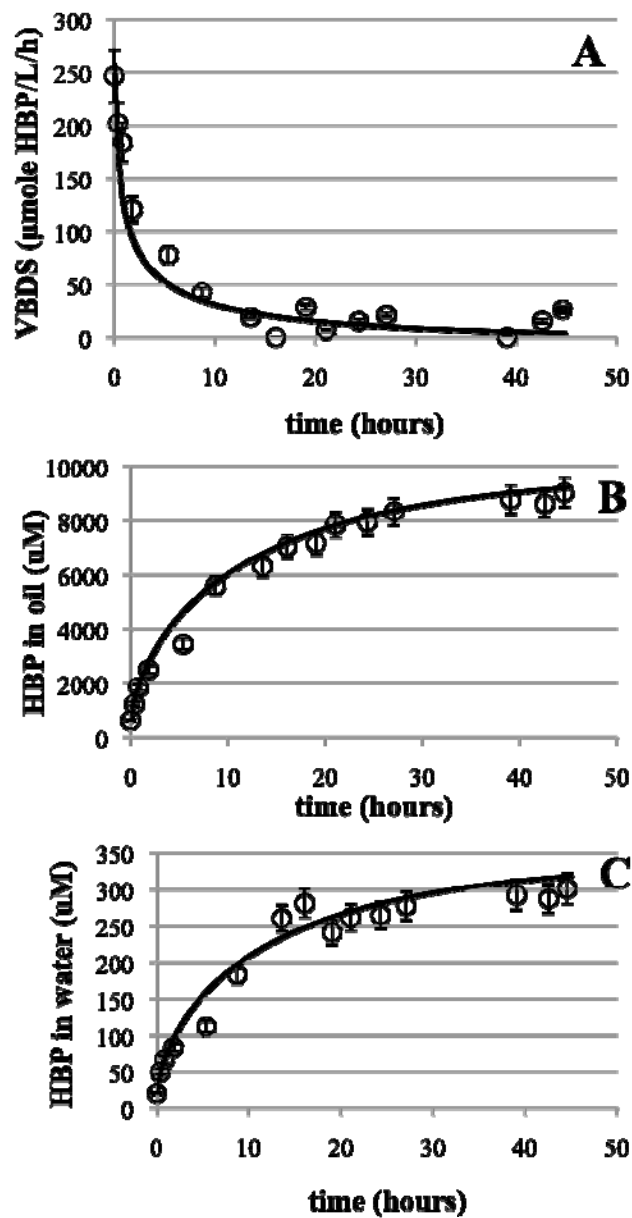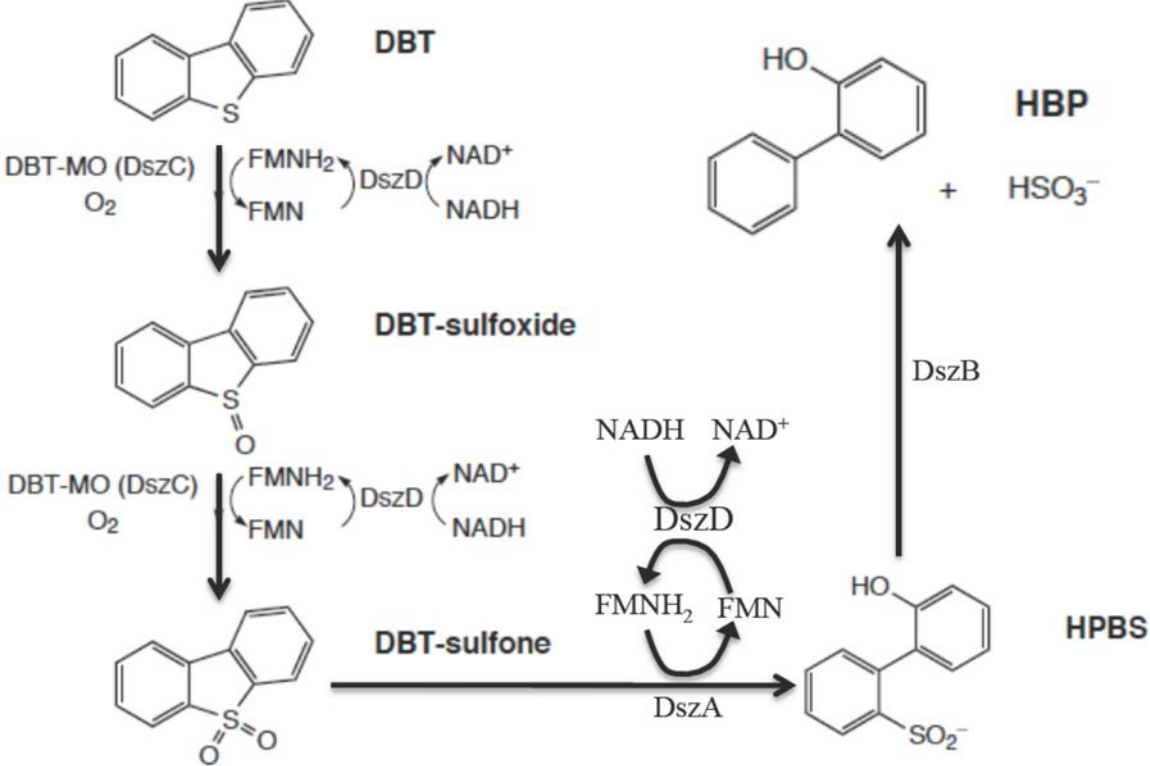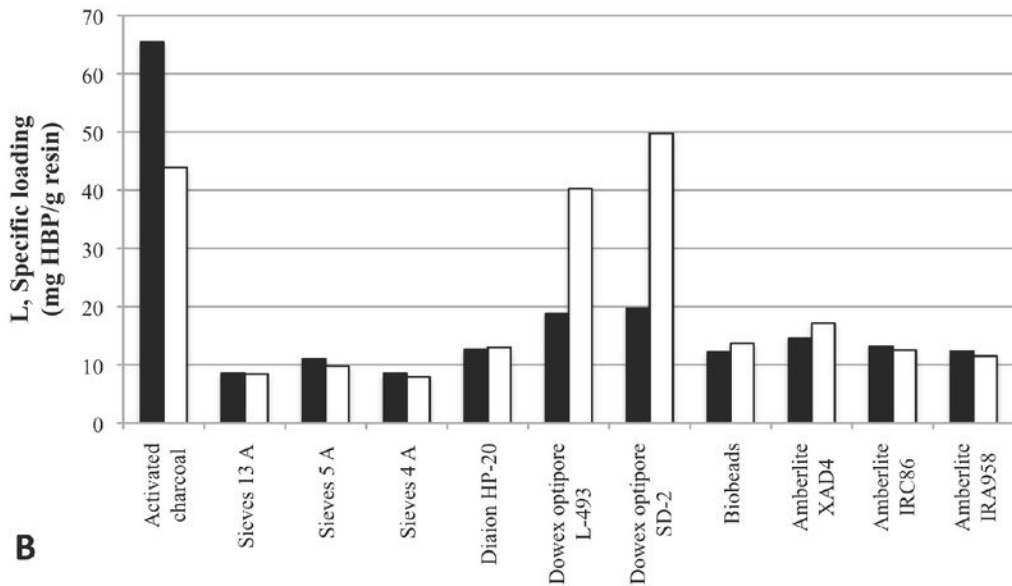
757

Figure 6. Enzyme inhibition model predictions for BDS bioreactor experiment. (A) – Volumetric desulfurization rate, V_{BDS}, data (circles) and model prediction (line). (B) – Concentration of HBP in the oil phase data (circles) and model (line). (C) – Concentration of HBP in the water phase data (circles) and model (line). Data shown are the average and standard deviations of 3 replicates.

758

759

A

B